J. Appl. Cryst. (1989). **22**, 26-34

Asymmetric X-ray Line Broadening of Plastically Deformed Crystals. II. Evaluation Procedure and Application to [001]-Cu Crystals

By T. Ungár and I. Groma

Institute for General Physics, Eötvös University, H-1445 Budapest, POB 323, Hungary

and M. Wilkens

Max-Planck-Institut für Metallforschung, Institut für Physik, 7000 Stuttgart 80, Federal Republic of Germany

(Received 2 May 1988; accepted 1 August 1988)

Abstract

In paper I [Groma, Ungár & Wilkens (1988). *J. Appl. Cryst.* **21**, 47-53] a theory was developed to interpret the asymmetric X-ray line broadening of plastically deformed crystals. It was shown that the dislocation structure can be described by five distinct parameters, namely the dislocation density, the mean quadratic spatial fluctuation of the dislocation density, the effective outer cut-off radius, the dipole polarization and the spatial fluctuation of the dipole polarization of the dislocation structure. In this paper a procedure is developed to evaluate these parameters from the Fourier transform of the line profiles. The theory and this procedure are tested by applying it to the asymmetric line profiles of tensile-deformed Cu single crystals orientated for ideal multiple slip. The asymmetry of these profiles is assigned to the dipole polarization of the dislocation cell structure and is directly correlated to residual long-range internal stresses. It is shown that the data can be interpreted in terms of the quasi-composite model of the dislocation cell structure developed earlier for the same material.

1. Introduction

In an earlier paper (Groma, Ungár & Wilkens, 1988, hereafter paper I) a theory was developed for the interpretation of the asymmetric X-ray line broadening of plastically deformed crystals. According to this theory the dislocation structure can be characterized by five different parameters: (i) the average dislocation density, ρ; (ii) the dipole polarization, P_0, of the dislocation structure; (iii) the so-called effective outer cut-off radius of dislocations, R_{eff}; (iv) the spatial fluctuation of the dislocation density, $\langle\rho^2\rangle-\langle\rho\rangle^2$; and (v) the spatial fluctuation of the dipole polarization P_1.

The aim of the present paper is to test this theory by applying it to the evaluation of asymmetric X-ray line broadening observed on tensile-deformed Cu single crystals oriented for ideal multiple slip.

The 200-type Bragg reflections of tensile-deformed [001]-orientated Cu single crystals were investigated in a number of recent papers (Ungár, Mughrabi, Rönnpagel & Wilkens, 1984; Ungár, Mughrabi & Wilkens, 1984; Wilkens, 1984; Mughrabi, Ungár, Kienle & Wilkens, 1986). Denoting the tensile direction of the samples by [001], one may describe the qualitative features of the asymmetry of the 200 Bragg reflections in the following way.

(i) The maxima of the diffraction peaks are shifted towards larger diffraction angles for the 002 reflections and in the opposite sense for the 020 and/or 200 reflections referred to the peak position of the virgin crystal.

(ii) The intensity distributions obtained from the tensile-deformed cyrstals are strongly asymmetric. The tails decay more slowly on the smaller diffraction angle side for the 002 reflections and *vice versa* for the 020 and/or 200 reflections.

In the theory developed in paper I the Fourier transform of the line profiles is developed into a logarithmic-series expansion in which the five parameters mentioned above are the coefficients of the expansion. The average dislocation density is determined from the 002 reflection on the one side and the 020 and 200 reflections on the other side in a straightforward manner.

The fluctuation of the dislocation density and the dipole polarization of the dislocation structure are interpreted in terms of the quasi-composite model of dislocation cell structures first developed by Mughrabi (1983) to describe the plastic behaviour of fatigued Cu single crystals.

2. The Fourier transform of X-ray line profiles

In paper I it was shown that within the formalisms of the kinematical scattering of X-rays and the linear elasticity theory of dislocations the Fourier coefficients, $A(n)$, of X-ray line profiles can be

0021-8898/89/010026-09$03.00

developed into a series as follows:

$$\ln A(n) = -\langle\rho^*\rangle n^2 \ln (R_{\text{eff}}/n) + \tfrac{1}{2}[\langle\rho^{*2}\rangle - \langle\rho^*\rangle^2] n^4 \ln (R_2/n) \ln (R_3/n) - i\langle S\rho^*\rangle n^3 \ln (R_1/n) - (i/2)[\langle S\rho^{*2}\rangle - 2\langle\rho^*\rangle\langle S\rho^*\rangle] n^5 \times \ln (R_4/n) \ln (R_5/n) + O(n^6), \quad (1)$$

where the Fourier variable n is a distance variable, extending in real space, parallel to the diffraction vector $\mathbf{g}$, ρ^* is the so-called formal value of the dislocation density and R_{eff} is the effective outer cut-off radius of the dislocation distribution. The radii R_1 to R_5 are parameters with the dimension of length which appear in the logarithmic series expansion and which will not be discussed in more detail here. The symbol $\langle\ \rangle$ stands for the averaging over a plane F in the crystal, extending perpendicular to a given set of straight dislocations

$$\langle \ldots \rangle = (1/F) \int_F \ldots \mathrm{d}^2\mathbf{r}. \quad (2)$$

The quantity S characterizes the dipole polarization of the dislocation structure and is defined as

$$S(\mathbf{r}) = \int \mathbf{P}(\mathbf{r}-\mathbf{v})\{\mathbf{e}[2\pi\, \partial^2\mathbf{g}/\partial\mathbf{v}\, \partial\mathbf{v}](\mathbf{v})\}\, \mathrm{d}^2\mathbf{v}, \quad (3)$$

where $\mathbf{P}$ is the dipole polarization density of dislocations, as defined in equation (29) of paper I; $\mathbf{u}$ is the displacement field of a single dislocation; $\mathbf{e}$ is a vector parallel to the (x, y) projection of $\mathbf{g}$, where the (x, y) plane is normal to the line vector, $\mathbf{l}$, of the dislocations, $|\mathbf{e}| = \sin\psi$, where ψ is the angle between $\mathbf{g}$ and $\mathbf{l}$; $\mathbf{r}$ and $\mathbf{v}$ are (two-dimensional) coordinates in the plane F. It is important to note that (1) is only valid for small values of n.

Equation (1) can be written in the form

$$\ln |A(n)| = n^2\rho^*[\ln n - C_1] + \tfrac{1}{2}\Delta\rho^{*2} n^4[\ln^2 n - C_2 \ln n + C_3] + O(n^6) \quad (4)$$

$$\operatorname{Arg}[A(n)] = n^3 P_0[\ln n - D_1] - \tfrac{1}{2} P_1 n^5[\ln^2 n - D_2 \ln n + D_3] + O(n^7), \quad (5)$$

where

$$\rho^* = \langle\rho^*\rangle \qquad \Delta\rho^{*2} = \langle\rho^{*2}\rangle - \langle\rho^*\rangle^2$$
$$C_1 = \ln R_{\text{eff}} \qquad D_1 = \ln R_1$$
$$C_2 = \ln (R_2 R_3) \qquad D_2 = \ln (R_4 R_5)$$
$$C_3 = \ln R_2 \ln R_3 \qquad D_3 = \ln R_4 \ln R_5.$$
$$P_0 = \langle S\rho^*\rangle$$
$$P_1 = \langle S\rho^{*2}\rangle - 2\langle\rho^*\rangle\langle S\rho^*\rangle$$

The parameters R_1 to R_5 will not be interpreted physically in the present case. Therefore we are allowed to eliminate the terms proportional to C_3 in (4) and D_3 in (5) by appropriate transformations. This will be demonstrated in the case of (4) in some detail. For this purpose we introduce an auxiliary function $f(n)$ according to the transformation

$$f(n) = \ln |A(n)| - \tfrac{1}{16} \ln |A(2n)| = \alpha_1\varphi_1(n) + \alpha_2\varphi_2(n) + \alpha_3\varphi_3(n) + \alpha_4\varphi_4(n) + O(n^6) \quad (6)$$

where

$$\varphi_1(n) = n^2 \ln n, \qquad \varphi_2(n) = n^2,$$
$$\varphi_3(n) = n^4 \ln n, \qquad \varphi_4(n) = n^4$$

and

$$\alpha_1 = \tfrac{3}{4}\rho^*, \qquad \alpha_2 = -\tfrac{3}{4}C_1\rho^* - \tfrac{1}{4}\rho^* \ln 2,$$
$$\alpha_3 = -\Delta\rho^{*2} \ln 2, \qquad \alpha_4 = -\tfrac{1}{2}\Delta\rho^{*2}[\ln^2 2 - C_2 \ln 2].$$

It has to be noted that after this transformation the power of $\ln n$ in the third and fourth terms on the right-hand side in (4) is reduced by one.

3. Evaluation procedure

3.1. *Evaluation of the absolute values of the Fourier coefficients*

It is important to note that the $O(n^6)$ part of the function in (6) becomes important at a rather fast rate as n increases. This means that the presence of the $O(n^6)$ term in (6) cannot be ignored during the determination of the $\alpha_1, \ldots, \alpha_4$ parameters. For this reason an evaluation procedure has been developed in which the $\alpha_1, \ldots, \alpha_4$ parameters are determined in such a way that the effect of the $O(n^6)$ term becomes negligibly small.

From the point of view of their behaviour in the vicinity of $n = 0$ the first four terms on the right-hand side of (6) can be divided into two subgroups. The first subgroup consists of the two terms proportional to $n^2 \ln n$ and n^2 which are the leading terms in this range. The second subgroup, which consists of the terms proportional to $n^4 \ln n$ and n^4, is proportional to $\Delta\rho^{*2}$ and is considered as a perturbation compared with the first subgroup.

According to this concept we determine first the coefficients α_1 and α_2 of the leading functional terms. The function $f(n)$ is fitted to the two leading functions φ_1 and φ_2 by the method of least squares as a function of the length of the fitting interval.

The least-squares fitting of $f(n)$ [*cf.* (6)] can be written as

$$\int_0^n \{f(n') - [a_1(n)\varphi_1(n') + a_2(n)\varphi_2(n')]\}^2\, \mathrm{d}n' = \min (a_1, a_2), \quad (7)$$

where the minimizing parameters are the $a_1(n)$ and

$a_2(n)$ functions. Inserting the theoretical expression of $f(n)$ [*cf.* (6)] into (7), one can obtain the theoretical form of the a_1 and a_2 functions:

$$\begin{aligned} a_1(n) &= \alpha_1 + \alpha_3 M_3(n) + \alpha_4 M_4(n) + O(n^4) \\ a_2(n) &= \alpha_2 + \alpha_3 N_3(n) + \alpha_4 N_4(n) + O(n^4), \end{aligned} \tag{8}$$

where

$$M_3(n) = n^2[(50/49)\ln n + 75/343], \tag{9}$$

$$M_4(n) = n^2(50/49), \tag{10}$$

$$N_3(n) = n^2[-(50/49)(\ln n)^2 + (240/343)\ln n - 20/343], \tag{11}$$

$$N_4(n) = n^2[-(50/49)\ln n + 45/49]. \tag{12}$$

Since the functions M_3, M_4, N_3 and N_4 tend to zero as $n \to 0$, the following can be written:

$$\lim_{n\to 0} a_i(n) = \alpha_i \quad i = 1, 2. \tag{13}$$

The evaluation of experimental data proceeds by inserting the experimentally determined $f(n)$ values into (7). A numerical least-squares evaluation of (7) provides experimental values of the functions $a_i(n)$ denoted by $a_i^e(n)$, $i = 1, 2$. The experimental values of the α_1 and α_2 parameters are obtained by extrapolating the $a_{1,2}^e(n)$ functions to $n = 0$. The extrapolation procedure is carried out by using the first three terms in the theoretical form of the functions $a_{1,2}(n)$ [*cf.* (8)-(12)].

In order to determine $\Delta\rho^{*2}$, the values of the parameters α_3 and α_4 have to be evaluated. Since the α_1 parameter was obtained by an extrapolation procedure it is reasonable to eliminate it from (8) by a more exact method, as follows:

$$\hat{a}_1(n) = a_1(n) - (1/n)\int_0^n a_1(n')\,dn'. \tag{14}$$

The same transformation of a_1^e gives the experimental function $\hat{a}_1^e(n)$. From (8) and (14),

$$\hat{a}_1(n) = \alpha_3 F_3(n) + \alpha_4 F_4(n) + O(n^4), \tag{15}$$

where

$$\begin{aligned} F_3(n) &= n^2[(100/147)\ln n + 25/147] \\ F_4(n) &= n^2(100/147). \end{aligned} \tag{16}$$

The α_3 and α_4 parameters are obtained in a similar way to α_1 and α_2 by the following least-squares fitting procedure:

$$\int_0^n \{\hat{a}_1^e(n') - [a_3(n)F_3(n') + a_4(n)F_4(n')]\}^2\,dn' = \min(a_3, a_4), \tag{17}$$

from which α_3 and α_4 are obtained as

$$\lim_{n\to 0} a_i(n) = \alpha_i \quad i = 3, 4. \tag{18}$$

Since $a_1(n)$ and $a_2(n)$ are not independent of each other $a_2(n)$ will not be analysed further.

3.2. *Evaluation of the argument of the Fourier coefficients*

The argument of the Fourier coefficients is sensitive to the origin of the Fourier transformation. If $A'(n)$ denotes the experimentally determined Fourier transform, which may refer to an incorrectly chosen origin, then it holds that

$$\mathrm{Arg}\,[A'(n)] = \mathrm{Arg}\,[A(n)] + kn, \tag{19}$$

where $\mathrm{Arg}\,[A(n)]$ is defined in (5) and k is a constant proportional to the difference between the origin of the Fourier transformation and the correct origin, *i.e.* the centre of gravity of the line profile. Experience has shown that the centre of gravity of a line profile can almost never be determined with the required accuracy. Nevertheless the term kn in (19) can be eliminated without changing the general structure of (5) by the transformation

$$g(n) = (1/n)\,\mathrm{Arg}\,[A'(n)] - (1/n)\int_0^{n'} (1/n')\,\mathrm{Arg}\,[A'(n')]\,dn'. \tag{20}$$

It turns out that $g(n)$, with $\mathrm{Arg}\,[A(n)]$ according to (5), is of exactly the same structure as $\ln|A(n)|$ in (4). Thus, the same transformation as shown in (6) can be applied to $g(n)$ in order to eliminate the term proportional to D_3. Subsequently, the parameters P_0, D_1, P_1 and D_2 in (5) can be obtained by the same numerical procedure as described in § 3.1.

4. An experimental test of the procedure

4.1. *Experimental*

The line profiles of the 002 and 020 Bragg reflections of a [001]-orientated Cu single crystal were investigated. The sample was tensile deformed up to the resolved shear stress value $\hat{\tau} = 75{\cdot}6$ MPa, referred to the eight equivalent slip systems {111}, ⟨110⟩ with non-vanishing Schmid factors. After deformation two types of samples were prepared from the bulk of the crystal, one with a plane surface perpendicular to the tensile axis ['axial case', (001) plane] and the other with a plane surface parallel to the tensile axis ['side case', (010) or (100) plane].

The intensity distributions of the 002 and 020 Bragg reflections are shown in Fig. 1, where $\theta = \theta_0 + \Delta\theta$ is the diffraction angle and θ_0 is determined by the centre of gravity of the Bragg reflection of the undeformed crystal. The figure indicates that the profiles are markedly asymmetric. The tails decay more slowly on the smaller-diffraction-angle side for the axial case and *vice versa* for the side case. More details of the qualitative features of these line profiles

have been described previously (Ungár, Mughrabi, Rönnpagel & Wilkens, 1984; Ungár, Mughrabi & Wilkens, 1984; Mughrabi, Ungár, Kienle & Wilkens, 1986).

The line profiles in Fig. 1 were measured with an achromatic double-crystal diffractometer installed in the laboratory of one of the present authors (TU) according to the principles described by Wilkens & Eckert (1964). Further experimental details have been described elsewhere (Ungár, Tóth, Illy & Kovács, 1986). It is worth mentioning that the profiles in Fig. 1 are equivalent to the corresponding profiles measured earlier on the same samples in the laboratory of Wilkens (Ungár, Mughrabi, Rönnpagel & Wilkens, 1984; Ungár, Mughrabi & Wilkens, 1984).

4.2. *Experimental results*

Fig. 2 shows the experimental functions $a_1^e(n)$ and $a_2^e(n)$ as determined from the least-squares evaluation of (7), as a function of n. The extrapolations of these functions to $n = 0$ yield for the axial case the following values for ρ^* and R_{eff} [*cf.* (6) and (13)]:

$$\rho^*_{002} = 5{\cdot}13 \times 10^{14}\ \text{m}^{-2}$$
$$R_{\text{eff}} = 0{\cdot}7 \times 10^{-7}\ \text{m}. \qquad (21)$$

The experimental function $a_3^e(n)$ obtained from the least-squares evaluation of (17) is shown in Fig. 2(*c*). The value of $\Delta\rho^{*2}$ can be obtained by the extrapolation of (18):

$$\Delta\rho^{*2} = 3{\cdot}14 \times 10^{29}\ \text{m}^{-4}. \qquad (22)$$

The same values for the side case are as follows:

$$\rho^*_{020} = 3{\cdot}59 \times 10^{14}\ \text{m}^{-2}$$
$$R_{\text{eff}} = 1{\cdot}02 \times 10^{-7}\ \text{m} \qquad (23)$$
$$\Delta\rho^{*2} = 2{\cdot}92 \times 10^{29}\ \text{m}^{-4}.$$

The values of P_0 and P_1 [*cf.* (5)] can be obtained from the imaginary part of the Fourier coefficient by carrying out a similar extrapolation procedure to the one described in (13) and (18) and shown in Fig. 3.

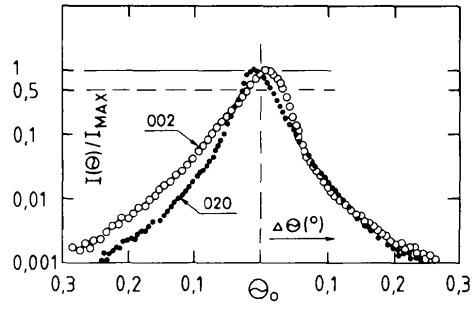

Fig. 1. The intensity distributions, $I(\theta)/I_{\max}$ ($\theta = \theta_0 + \Delta\theta$) of the 002 and 020 Bragg reflections of tensile-deformed Cu single crystals oriented for ideal multiple slip, $\hat{\tau} = 75{\cdot}6$ MPa. θ_0 is determined as the centre of gravity of $I(\theta)$.

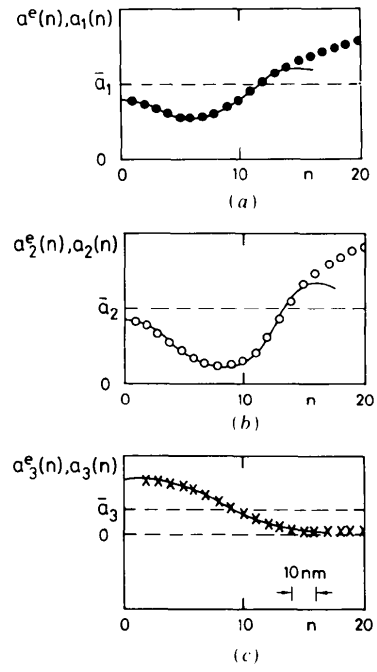

Fig. 2. The functions $a_1^e(n)$ (●), $a_2^e(n)$ (○) and $a_3^e(n)$ (×) defined by equations (7) and (17), respectively. The dashed lines in (*a*) and (*b*) which are the average values of $a_1^e(n)$ and $a_2^e(n)$ within the n range indicated in the figure give the scaling units of the ordinate axis. The solid curves drawn through the data points indicate the a_1, a_2, a_3 theoretical fitting functions given by equations (8) and (17).

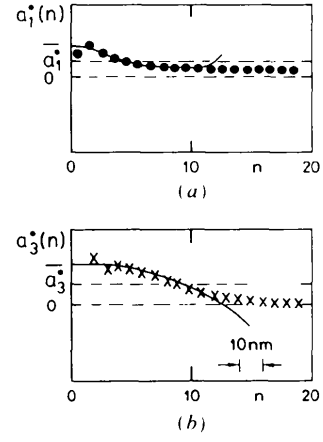

Fig. 3. The imaginary part of the Fourier coefficients is represented by the $g(n)$ function given in equation (20). The $g(n)$ function can be evaluated by exactly the same procedure as $f(n)$ in equation (6). If one denotes the corresponding auxiliary functions by $a_1^*(n)$, $a_3^*(n)$ in an analogous manner to equations (7), (8), (17) and Fig. 2, the indicated data points give the experimental values, analogously to equations (7) and (17). The solid lines drawn through the data points give the theoretical fitting functions similarly to those given by equation (8) for the real part of the Fourier coefficients. The P_0 and P_1 values are obtained from the extrapolated values of a_1^* and a_3^* to $n = 0$. The $\bar{a}_1^*$ and $\bar{a}_3^*$ values in (*a*) and (*b*) are the average values of the data points within the n range given in the figure which give the scaling units of the ordinate axis.

Table 1. *Geometrical factors of X-ray line broadening for* 002 *reflections (Wilkens,* 1987)

l	b	γ (°)	g	c
112	$\bar{1}10$	90	200	0·4303
			002	0·0667
			200	0·2732
110	101	60	002	0·4726
			020	0·0996

l Line vector; **b** Burgers vector; **g** diffraction vector; γ angle between **l** and **b**.

The numerical results are the following for the axial case:

$$P_0 = -2{\cdot}97 \times 10^{21}\ \mathrm{m}^{-3}$$
$$P_1 = 9{\cdot}02 \times 10^{36}\ \mathrm{m}^{-5}, \tag{24}$$

and for the side case:

$$P_0 = 8{\cdot}59 \times 10^{20}\ \mathrm{m}^{-3}$$
$$P_1 = -1{\cdot}85 \times 10^{36}\ \mathrm{m}^{-5}. \tag{25}$$

The true values of the dislocation density, ρ, can be obtained from ρ^* by the following expression [*cf.* Wilkens (1970*a*) and equation (41) of paper I]:

$$\rho = (2/\pi)\rho^*/g^2b^2C \tag{26}$$

where g and b are the absolute values of the diffraction and the Burgers vectors, respectively. C is a geometrical factor which depends on the correlation between the line and Burgers vectors, **l** and **b**, and the diffraction vector, **g**. For the anisotropic case of pure copper C was evaluated by Wilkens (1987). The C data relevant to the present case are listed in Table 1.

The averaging of the geometrical parameters was performed in a similar way to that described in a previous account (Ungár, Mughrabi, Rönnpagel & Wilkens, 1984) by assuming that: (i) those eight slip systems which are activated with non-vanishing Schmid factors are counted with equivalent weight factors; (ii) all dislocations are of edge or 60° character with equal probability; and (iii) the slip systems with zero Schmid factors, *i.e.* those for which **b** is perpendicular to the tensile axis, are taken into account with a weight factor φ.

The last assumption is suggested by the transmission electron microscopy (TEM) results of Göttler (1973), according to which the frequency of such types of dislocations is considerable.

Denoting the ratio ρ^*/ρ by Q, we find that the average values of Q can be obtained from the assumptions (i) to (iii) for the axial and side cases, respectively. With the geometric factors listed in Table 1 and with the postulate that the 'true' value of ρ should be the same for the axial and the side case, respectively, the values of Q are as follows:

$$\bar{Q}_{002} = (5{\cdot}042 + 0{\cdot}5215\varphi)/(4 + 2\varphi) \tag{27}$$

$$\bar{Q}_{020} = (2{\cdot}729 + 2{\cdot}83\varphi)/(4 + 2\varphi). \tag{28}$$

With the ρ^* values in (21) and (23) the average dislocation density ρ and the weight factor φ are

$$\rho = 4{\cdot}58 \times 10^{14}\ \mathrm{m}^{-2}$$
$$\varphi = 0{\cdot}32. \tag{29}$$

The experimental data in this section are given to three digits for the purpose of identification. The experimental error in determining ρ^*, $\Delta\rho^*$ and P_0 is, however, about ±10%.

5. The interpretation of the data in terms of the composite model of the dislocation cell structure

In a number of previous papers it was shown that the plastic behaviour of tensile-deformed [001]-orientated copper single crystals can be described in terms of a composite model (Mughrabi, 1983; Ungár, Mughrabi, Rönnpagel & Wilkens, 1984; Mughrabi, Ungár & Wilkens, 1986). The cell walls and cell interiors are considered as spatially alternating 'hard' and 'soft' regions of the material. Upon uniaxial loading the two regions are strained in a more or less parallel switched mode. Upon subsequent unloading the plastic strain mismatch between the soft cell interiors and the hard cell walls is balanced by the evolution of long-range internal stresses which put the cell walls under an extra tensile and the cell interiors under an extra compressional stress.

This means that the dislocation structure and the internal stresses are space dependent with two distinct values. In the following the values corresponding to the cell walls and cell interiors will be distinguished by the subscripts w and c, respectively. The volume fraction of the cell walls will be denoted by f.

According to (3), the parameters which are relevant for the present considerations in (4) and (5) can be written as

$$\rho = f\rho_w + (1-f)\rho_c \tag{30}$$

$$\Delta\rho^2 = f(1-f)(\rho_w - \rho_c)^2 \tag{31}$$

$$P_0 = fS_w\rho_w + (1-f)S_c\rho_c \tag{32}$$

$$P_1 = fS_w\rho_w^2 + (1-f)S_c\rho_c^2 - 2\rho P_0. \tag{33}$$

According to equation (53) of paper I the following relation is valid:

$$fS_w + (1-f)S_c = 0. \tag{34}$$

The system of equations in (30) to (34) determines the values of ρ_w, ρ_c, S_w, S_c and f.

From the data in (21) to (25) the following values are obtained:

$$\rho_w = 12{\cdot}23 \times 10^{14}\ \mathrm{m}^{-2}$$
$$\rho_c = 1{\cdot}31 \times 10^{14}\ \mathrm{m}^{-2}$$
$$S_w = -8{\cdot}1 \times 10^{6}\ \mathrm{m}^{-1} \tag{35}$$
$$S_c = 3{\cdot}47 \times 10^{6}\ \mathrm{m}^{-1}$$
$$f = 0{\cdot}3.$$

6. Comparison of the present procedure with the subdivision of the asymmetric profiles into two symmetric subprofiles

In order to find a direct correlation between the present evaluation procedure and the earlier evaluation based on the quasi composite concept of the dislocation cell structure (*cf.* Ungár, Mughrabi, Rönnpagel & Wilkens, 1984; Mughrabi, Ungár, Kienle & Wilkens, 1986) the Fourier coefficients have to be presented in a form which is an intermediate step in the theory [equation (54) of paper I]. According to this equation $A(n)$ can be written as

$$A(n) = (1/F) \int_F \exp\{-\rho^*(\mathbf{r}) n^2 \ln [R_e(\mathbf{r})/n] - iS(\mathbf{r})n\} \, d^2\mathbf{r}. \quad (36)$$

In terms of the composite model of the dislocation cell structure the integral above becomes the sum of two terms,

$$A(n) = A_w(n) + A_c(n), \quad (37)$$

where

$$A_w(n) = f \exp[-\hat{C}\rho_w n^2 \ln(R_{ew}/n) - iS_w n]$$
$$A_c(n) = (1-f) \exp[-\hat{C}\rho_c n^2 \ln(R_{ec}/n) - iS_c n],$$

with $\hat{C} = (\pi/2) g^2 b^2 C$ [*cf.* (26)].

The reversed Fourier transform of $A(n)$ yields two symmetric subprofiles which are shifted with respect to the centre of gravity by S_w and S_c, respectively. The integral intensity of the subprofiles is $f = A_w(0)/A(0)$ and $(1-f) = A_c(0)/A(0)$ respectively.

In previous papers the asymmetric profiles were evaluated by subdividing them into the sum of two symmetric subprofiles (Ungár, Mughrabi, Rönnpagel & Wilkens, 1984; Mughrabi, Ungár, Kienle & Wilkens, 1986). Equations (36) and (37) indicate that this evaluation is equivalent to the interpretation of the data obtained from the present procedure in terms of the composite model.

In a number of previous accounts it was shown that S_w and S_c give a measure of the elastic change of the lattice plane spacings in the cell walls and cell interiors, respectively (Ungár, Mughrabi, Rönnpagel & Wilkens, 1984; Ungár, Mughrabi & Wilkens, 1984). These tetragonal lattice distortions indicate the existence of residual long-range internal stresses which can be obtained as follows:

$$\Delta\tau_w = -(S_w/g)\varphi E$$
$$\Delta\tau_c = -(S_c/g)\varphi E, \quad (38)$$

where $g = 2 \sin\theta_0/\lambda$, θ_0 is the exact Bragg angle, λ is the wavelength of the X-radiation, φ is the Schmid factor, $\varphi = 0{\cdot}408$ for the present case, and $E = 6{\cdot}7 \times 10^4$ MPa is Young's modulus. The data in (35) give the following values for the long-range internal stresses:

$$\Delta\tau_w = 40{\cdot}5 \text{ MPa}$$
$$\Delta\tau_c = -17{\cdot}4 \text{ MPa}. \quad (39)$$

7. Discussion

7.1. *On the evaluation of dislocation densities*

In § 4.1 the average dislocation density of a tensile deformed [001]-orientated Cu single crystal was determined by the analysis of the Fourier coefficients of the X-ray line profiles. The main steps of the procedure are given in (4), (6), (7) and (14). The evaluation was carried out on both, the 002 'axial' and the 020 'side' reflections which are asymmetric in the opposite sense, as shown in Fig. 1.

The formal value of the dislocation density, ρ^*, was found to be larger for the axial case than for the side case. Obviously the true dislocation densities observed by the two different reflections must be the same. This enabled the determination of the population of Burgers vectors on the different slip systems. With the assumption that the eight equivalently activated slip systems have a uniform population of Burgers vectors and that the four unactivated slip systems are populated with the weight factor φ, φ was obtained to be 0·32. This means that the Burgers vector population on the unactivated slip systems is about 32% compared with the population of the activated slip systems. About the same population of non-activated Burgers vectors was observed by Göttler (1973) by TEM investigations. It is important to note that this is a non-trivial result of the present evaluation procedure. In a previous account the asymmetric profiles were decomposed into the sum of the so-called 'well behaved' symmetric subprofiles (Ungár, Mughrabi, Rönnpagel & Wilkens, 1984). The subprofiles were assigned to the alternating regions of high and low local dislocation density, *i.e.* to the cell walls and cell interiors of the dislocation cell structure. The local dislocation densities were obtained from the subprofiles by the application of Wilkens's (1970*a*, *b*) theory. This was done, however, only for the 002 axial case, since for the 020 side case reflections (i) the decomposition procedure was less reliable due to the smaller scale of asymmetry and (ii) these subprofiles yielded unrealistic values for the local dislocation densities. For more details of these difficulties the reader is referred to Ungár, Mughrabi, Rönnpagel & Wilkens (1984).

7.2. *Correlation between the dipole polarization of the dislocation structure and the long-range internal stresses*

The dipole-polarization density of the dislocation structure, $\mathbf{P}(\mathbf{r})$, was defined by equation (29) of paper I. As is clear from this definition, $\mathbf{P}(\mathbf{r})$ has a strong

correlation with the difference between the distribution functions of dislocations of opposite sign. However, as was shown in paper I and indicated by (3) and (5), the Fourier coefficients deliver primarily the quantity S. In a sense S could be called the 'formal' value of the dipole-polarization density, just as ρ^* is called the formal value of the dislocation density. In order to obtain $\mathbf{P}(\mathbf{r})$ from the S values, (3) would have to be solved for a particular dislocation model. At the present state of the art we satisfy ourselves, however, by interpreting the S values in terms of the composite model of dislocation cell structures, as was done in §§ 5 and 6.

On the other hand, it is easy to give a qualitative microscopic picture for $\mathbf{P}$, which is also based on the composite model of dislocation cell structures. As was described earlier, upon plastic straining, the plastic-strain mismatch between the soft cell interiors and the hard cell walls is accommodated by the accumulation of geometrically necessary dislocations at the interfaces between cell walls and cell interiors (Ungár, Mughrabi, Rönnpagel & Wilkens, 1984; Ungár, Mughrabi & Wilkens, 1984). The geometrically necessary dislocations on either side of the cell walls (and/or on either side of the cell interiors) are totally polarized dislocation dipoles whose dipole-polarization density has to be given by the $\mathbf{P}(\mathbf{r})$ function.

The geometrically necessary dislocation dipoles are the sources of the residual long-range internal stresses which can be directly deduced from the values of S, as shown in § 5.

The evaluation of (3) for a suitable model would provide the density and distribution of the geometrically necessary dislocation dipoles.

7.3. *The fluctuation of the dislocation density*

The mean quadratic fluctuation of the dislocation density, $\Delta\rho^2$, is one of the most remarkable parameters provided by the present theory. Equation (1) indicates that it is independent of the asymmetry of a profile. In terms of the composite model of dislocation cell structures it was interpreted as a measure of the difference in dislocation densities between the cell walls and cell interiors [*cf.* (4) and the notations listed below].

The values of ρ_w and ρ_c given in (35) are somewhat higher and lower, respectively, than the ρ_w and ρ_c values obtained previously for the same material (Ungár, Mughrabi & Wilkens, 1984); *cf.* § 7.4. The ratio ρ_w/ρ_c in the present case is close to 10. Previously this ratio was found to be about 5 (Ungár, Mughrabi & Wilkens, 1984). The present result is more satisfying if compared with the TEM micrographs of the cell structure (Ungár, Mughrabi & Wilkens, 1984; Mughrabi, Ungár, Kienle & Wilkens, 1986). The relatively low value of this ratio, found previously, was explained by the fact that, by decomposing the asymmetric profiles into two symmetric subprofiles, the profiles related to the cell-interior material contain the contribution from the cell-wall material which is lying more or less perpendicular to the tensile axis. This effect increases ρ_w and hence reduces ρ_c. The present evaluation procedure is obviously free from this type of error.

Table 2. *The local dislocation densities, ρ_w and ρ_c, the total dislocation density, ρ_t, in units of 10^{14} m^{-2}, and the long-range internal stresses in the cell walls and cell interiors after unloading, $\Delta\tau_w$ and $\Delta\tau_c$, in units of* MPa

All data refer to the applied stress $\hat{\tau} = 75{\cdot}6$ MPa.

	Type of reflection	ρ_w	ρ_c	ρ_t	$\Delta\tau_w$	$\Delta\tau_c$
Previous results*	002	7·9	1·56	3·46	51·4	−17·2
Present results	002 and 020	12·23	1·31	4·58	40·5	−17·4

* Ungár, Mughrabi, Rönnpagel & Wilkens (1984).

From (32) and (34) the following relation can be derived:

$$P_0/[f(1-f)] = (S_w - S_c)(\rho_w - \rho_c). \qquad (40)$$

This relation indicates that in a homogeneous dislocation structure, *i.e.* if $\rho_w - \rho_c = 0$, P_0 vanishes and the line profiles remain symmetric up to higher-order terms proportional to n^5; *cf.* the term proportional to P_1 in (5).

7.4. *Comparison of the results obtained by the present method and the decomposition procedure of asymmetric profiles into symmetric subprofiles*

In previous papers the local dislocation densities, ρ_w and ρ_c, the total dislocation density, ρ_t, and the long-range internal stresses prevailing after unloading in the cell walls and in the cell interiors, $\Delta\tau_w$ and $\Delta\tau_c$, were obtained from the line-profile analysis of the symmetric subprofiles and from the shifts of the subprofiles relative to the centre of gravity of the measured profiles, respectively (*cf.* Ungár, Mughrabi, Rönnpagel & Wilkens, 1984; Ungár, Mughrabi & Wilkens, 1984; Mughrabi, Ungár, Kienle & Wilkens 1986). As was mentioned in paper I and also in the present work the ρ_i data ($i = w$, c or t) were obtained in these earlier papers from the profiles corresponding to the 'axial case', *i.e.* the 002 Bragg reflection. These data are given in the first row of Table 2.

Taking into account that: (i) the actual values of dislocation densities have a natural physical uncertainty, (ii) the previous and the present line profiles were measured in two different X-ray laboratories and (iii) the evaluation methods for the previous and present results are based on different concepts, the agreement of the corresponding data is fairly good.

The effective outer cut-off radii corresponding to the cell wall and to the cell-interior material, *i.e.* R_w and R_c respectively, were obtained by Ungár, Mughrabi, Rönnpagel & Wilkens (1984) from the symmetric subprofiles. These data are compared with R_{eff} given in (21) as follows. Let us expand (37) up to quadratic terms in n and set the sum of these two quadratic terms equal to the corresponding quadratic term in (1); then the following can be obtained:

$$R_{\text{eff}} = R_w^{f\rho_w/\rho_t} R_c^{(1-f)\rho_c/\rho_t}. \tag{41}$$

If we take the values of R_w and R_c from Table 2 then from Ungár, Mughrabi, Rönnpagel & Wilkens (1984), the value of R_{eff} for $g = 002$ and $\hat{\tau} = 75{\cdot}6$ MPa is obtained as

$$R_{\text{eff}} = 0{\cdot}72 \times 10^{-7} \text{ m}.$$

This value compares almost exactly with the value given in (21).

7.5. *On the accuracy of line-profile measurements required for the present evaluation procedure*

In § 3 it was shown that the parameters describing the dislocation structure can be divided into two classes in terms of the structure of the functions in the series expansion of (1). The leading terms in the series expansion give the dislocation density, the effective outer cut-off radius R_{eff} and the dipole polarization P_0. The higher-order terms provide the fluctuations of ρ and P_0, *i.e.* the terms $\Delta\rho^2$ and P_1. Owing to the sensitivity of these parameters to the exact shape of the line profiles, down to intensities $I(\theta)/I(\theta_0) \simeq 10^{-3}$, it is important to be able to measure $I(\theta)$ with an apparatus of high resolution power. This requirement is met by the double-crystal diffractometer with self-compensation of wavelength dispersion and negligible instrumental line broadening described by Wilkens & Eckert (1964). The line profiles in Fig. 1 were measured by this type of instrument with an instrumental line broadening of about 0·002° measured in θ.

7.6. *A note on the mathematics of the evaluation procedure*

In principle the quantities characterizing the dislocation structure could have been obtained by a simple least-squares fitting procedure by fitting (1) [or equation (57) of paper I] to the experimentally determined Fourier coefficients for small values of n. In fact this method of evaluation was tried at first. It turned out very soon, however, that the functions to which the fitting procedure would have to be applied belong to a very similar, if not the same, class of functions which makes a simple fitting procedure rather uncertain. If one takes, for example, the real part of the Fourier coefficients this means that in a simple parameter-fitting procedure the actual values of ρ^* and $\Delta\rho^{*2}$ would depend strongly on the number of Fourier coefficients for which the fitting was carried out. This dependence was found to be such that if ρ^* became larger then $\Delta\rho^{*2}$ became smaller and *vice versa*. In other words, the mixing of the first two functions in the series expansion of the real part of the Fourier coefficients (and in the imaginary parts too) cannot be carried out without special precautions.

A conventional plot of $A(n)$ *vs* n with both the experimental and the 'theoretical' values would be instructive. This cannot be done in a simple manner, however, since the parameters R_2, R_3, R_4 and R_5 in (1) were not determined. These are auxiliary length parameters which were not interpreted physically in the present case. Another possibility would be to compare the experimental values of $f(n)$ on the left side with the theoretical values on the right side of (6). Owing to the unknown higher-order terms this is still not a trivial matter. An appropriate comparison of the experimental and theoretical Fourier coefficients will be drawn, however, in a forthcoming paper.

8. Concluding remarks

A procedure has been developed to evaluate the asymmetrically broadened X-ray line profiles corresponding to plastically deformed crystals containing a fairly general distribution of dislocations. The dislocation structure is characterized by the following parameters: (i) the average dislocation density, ρ; (ii) the mean quadratic fluctuation of the dislocation distribution, $\Delta\rho^2 = \langle\rho^2\rangle - \langle\rho\rangle^2$; (iii) the dipole polarization of the dislocation structure, S; (iv) the effective outer cut-off radius of dislocations, R_{eff}; and (v) the fluctuation of the dipole polarization, $\langle S\rho^2\rangle - 2\langle\rho\rangle\langle S\rho\rangle$.

The procedure has been tested by evaluating the asymmetrically broadened line profiles of tensile-deformed [001]-Cu single crystals.

The parameters (i) to (v) were interpreted in terms of the quasi-composite model of dislocation cell structures developed earlier (Ungár, Mughrabi, Rönnpagel & Wilkens, 1984; Ungár, Mughrabi & Wilkens, 1984; Mughrabi, Ungár, Kienle & Wilkens, 1986).

The authors are indebted to Professor I. Kovács for his continuous and stimulating support during this work. Many thanks are due to Mr I. Puppán for his kind assistance in carrying out the X-ray measurements.

References

GÖTTLER, E. (1973). *Philos. Mag.* **28**, 1057–1076.
GROMA, I., UNGÁR, T. & WILKENS, M. (1988). *J. Appl. Cryst.* **21**, 47–53.
MUGHRABI, H. (1983). *Acta Metall.* **31**, 1367–1379.

MUGHRABI, H., UNGÁR, T., KIENLE, W. & WILKENS, M. (1986). *Philos. Mag. A*, **53**, 793-813.

MUGHRABI, H., UNGÁR, T. & WILKENS, M. (1986). *Z. Metallkd.* **77**, 571-575.

UNGÁR, T., MUGHRABI, H., RÖNNPAGEL, D. & WILKENS, M. (1984). *Acta Metall.* **32**, 333-342.

UNGÁR, T., MUGHRABI, H. & WILKENS, M. (1984). *Microstructural Characterization of Materials by Non-Microscopical Techniques*, edited by N. H. ANDERSEN, M. ELDRUP, N. HANSEN, D. JUUL JENSEN, T. LEFFERS, H. LILHOLT, O. B. PEDERSEN & B. N. SINGH, pp. 539-544. Risø National Laboratory, Roskilde, Denmark.

UNGÁR, T., TÓTH, L. S., ILLY, J. & KOVÁCS, I. (1986). *Acta Metall.* **34**, 1257-1267.

WILKENS, M. (1970*a*). In *Fundamental Aspects of Dislocation Theory*, edited by J. A. SIMMONS, R. DE WIT & R. BULLOUGH, Vol. II. pp. 1195-1221. *Natl Bur. Stand. (US) Spec. Publ.* No. 317. Washington, DC, USA.

WILKENS, M. (1970*b*). *Phys. Status. Solidi A*, **2**, 359-370.

WILKENS, M. (1984). *Microstructural Characterization of Materials by Non-Microscopical Techniques*, edited by N. H. ANDERSEN, M. ELDRUP, N. HANSEN, D. JUUL JENSEN, T. LEFFERS, H. LILHOLT, O. B. PEDERSEN & B. N. SINGH, pp. 153-168. Risø National Laboratory, Roskilde, Denmark.

WILKENS, M. (1987). *Phys. Status Solidi A*, **104**, K1.

WILKENS, M. & ECKERT, K. (1964). *Z. Naturforsch. Teil A*, **19**, 459-470.